Theor Chem Acc (2011) 130:51–60
DOI 10.1007/s00214-011-0958-0

REGULAR ARTICLE

# Mechanism and kinetics of the hydroxyl and hydroperoxyl radical scavenging activity of *N*-acetylcysteine amide

**Annia Galano**

Received: 5 April 2011 / Accepted: 7 May 2011 / Published online: 22 May 2011


**Abstract** The $^{\cdot}OH$ and $^{\cdot}OOH$ radical scavenging activity of *N*-acetylcysteine amide (NACA) has been studied using density functional theory, specifically the M05-2X functional. All possible reaction sites have been considered, and the branching ratios have been estimated. The efficiency of different mechanisms of reaction has been evaluated, and it has been concluded that NACA reacts exclusively by hydrogen atom transfer (HAT). The overall reactivity of NACA toward OH radicals is proposed to be diffusion-controlled in both non-polar and polar media. The values of the overall rate coefficients are $3.80 \times 10^9$ and $1.36 \times 10^9$ L $mol^{-1}$ $s^{-1}$ for benzene and aqueous solutions, respectively. The reactivity of NACA toward $^{\cdot}OOH$, on the other hand, is much lower but still higher than those of melatonin and caffeine. HAT from the –SH site is proposed to be the channel accounting for most of the radical scavenging activity of NACA in aqueous solution. In non-polar environments, two channels of reaction were found to similarly contribute to the overall reactivity of NACA toward OH radicals. They are those corresponding to hydrogen atom transfer from $–CH_2$ and –SH sites.

**Keywords** NACA · Oxidative stress · Free radicals · Antioxidant · Scavenger · Rate constant · Mechanisms

**Electronic supplementary material** The online version of this article (doi:10.1007/s00214-011-0958-0) contains supplementary material, which is available to authorized users.

A. Galano (✉)
Departamento de Química, División de Ciencias Básicas e Ingeniería, Universidad Autónoma Metropolitana-Iztapalapa,
Av San Rafael Atlixco No.186,
Col., 09340 Vicentina,
DF, México
e-mail: agal@xanum.uam.mx

## 1 Introduction

*N*-Acetylcysteine amide (NACA), also known as AD4, is a newly designed amide form of *N*-acetylcysteine (NAC), which has been proposed to efficiently fight oxidative stress (OS) [1–6]. This chemical stress arises from the imbalance between production and the consumption of reactive oxygen species (ROS) [7], and it has been proven to be involved in the development of a large variety of health disorders [8–14]. Since OS involves reactions between biological molecules and free radicals, the study of compounds with free radical scavenging activity becomes an important area of research aiming to prevent oxidative stress and the consequent molecular damage.

Grinberg et al. [1] have shown that NACA defend red blood cells from oxidation and proposed that it could be explored for the treatment of neurodegeneration and other oxidation-mediated disorders. Almost simultaneously, Penugonda et al. [2] have demonstrated that NACA can protect cells against glutamate cytotoxicity by inhibiting lipid peroxidation and scavenging ROS. In a following paper from the same group [15], it was described that NACA has also a protective role against the combined toxic effects of glutamate and lead by inhibiting lipid peroxidation and scavenging ROS, supporting their previous findings. Price et al. [3] found that oxidatively challenged cells were protected by NACA and that this compound blocked ROS generation. These authors also found that the oxidative stress induced by HIV-1 viral proteins can be effectively blocked by NACA. Wu et al. [4] have shown that NACA is superior to NAC as an antioxidant thiol radioprotector. They also found that while NAC can be cytotoxic to cells at high concentrations, at similar concentrations, NACA is non-toxic. Therefore, they proposed that NACA can be considered a promising agent to

be used as a supplement in situations that require protection from ionizing radiation. Very recent results also support the efficiency of NACA as antioxidant and lead to the proposal that this compound should be evaluated for the treatment of neurodegenerative diseases in the future [5]. Moreover, it has been tested whether NACA can protect the blood–brain barrier from oxidative stress–induced damage in animals, and it has been found that this compound is actually able to do such desirable action [6].

Another important characteristic of NACA is that while NAC does not readily permeate membranes by diffusion because it is negatively charged under physiological conditions, NACA is more able to permeate biological membranes since it has the carboxyl group replaced by an amide group, and therefore, this molecule remains uncharged under the same conditions [16, 17].

Based on all this experimental evidence, it can be concluded that NACA can efficiently fight OS. Therefore, it becomes important to investigate the mechanism, or mechanisms, involved in such process. To that end, it is the main goal of the present work to study different alternative mechanisms usually associated with the free radical scavenging activity of antioxidants. The studied mechanisms are radical adduct formation (RAF), hydrogen atom transfer (HAT), single electron transfer (SET), sequential electron proton transfer (SEPT), and proton-coupled electron transfer (PCET). They have all been studied for the reaction of NACA with hydroxyl ($^{\cdot}$OH) and hydroperoxyl ($^{\cdot}$OOH) radicals. Thermodynamic and kinetic data are provided, as well as the contributions of the different mechanisms to the OH and OOH free radical scavenging activity of NACA. This new information is expected to contribute to the better understanding of the protective role of NACA against OS.

## 2 Computational details

Geometry optimizations and frequency calculations have been carried out using the M05-2X functional and the 6-311++G(d,p) basis set. The M05-2X functional has been recommended for kinetic calculations by their developers [18], and it has been also successfully used by independent authors [19–27]. Moreover, the reliability of the kinetic data obtained with this functional, for radical-molecule reactions, has been proven by comparison with experimental data in numerous occasions [28–30]. Moreover, it has been demonstrated that in some cases, the correspondence between M05-2X and experimental results is better than the one obtained using highly correlated wave function methods [19, 21].

Unrestricted calculations were used for open shell systems, and local minima and transition states were identified by the number of imaginary frequencies (NIMAG = 0 or 1, respectively). Intrinsic reaction coordinate (IRC) calculations have been made to confirm that the transition states properly connect reactants and products. All electronic calculations were made with Gaussian 09 package of programs [31]. Thermodynamic corrections at 298 K were included in the calculation of relative energies. All calculations were made in solution, with the SMD continuum model [32], and using benzene and water as solvents, to mimic non-polar and polar environments, respectively. Benzene has been chosen because of its dielectric constant ($\varepsilon = 2.27$), which is similar to that of the hydrophobic region of bilayer membranes. Although there is some uncertainty about the actual value of $\varepsilon$ for the hydrocarbon region of a bilayer, a value $\sim$2.1 seems to be reasonable [33–35]. In fact, benzene is frequently used in both experimental [36–38] and theoretical [39–41] investigations to represent non-polar regions. The solvent cage effects have been included according to the corrections proposed by Okuno [42], taking into account the free volume theory [43]. These corrections are in good agreement with those independently obtained by Ardura et al. [44] and have been successfully used by other authors [45–51].

The rate constants ($k$) were calculated using conventional transition state theory (TST) [52–54] and 1 M standard state as:

$$k = \sigma\kappa\frac{k_B T}{h}e^{-(\Delta G^{\neq})/RT} \quad (1)$$

where $k_B$ and $h$ are the Boltzmann and Planck constants, $\Delta G^{\neq}$ is the Gibbs free energy of activation, $\sigma$ represents the reaction path degeneracy, accounting for the number of equivalent reaction paths, and $\kappa$ accounts for tunneling corrections. The tunneling corrections defined as the Boltzmann average of the ratio of the quantum and the classical probabilities were calculated using the Eckart barrier [55].

Some of the calculated rate constant ($k$) values are close to the diffusion-limited rate constant. Accordingly, the apparent rate constant ($k_{app}$) cannot be directly obtained from TST calculations. In the present work, the Collins–Kimball theory is used for that purpose [56]:

$$k_{app} = \frac{k_D k_{act}}{k_D + k_{act}} \quad (2)$$

where $k_{act}$ is the thermal rate constant, obtained from TST calculations (Eq. 1), and $k_D$ is the steady-state Smoluchowski [57] rate constant for an irreversible bimolecular diffusion-controlled reaction:

$$k_D = 4\pi R D_{AB} N_A \quad (3)$$

where $R$ denotes the reaction distance, $N_A$ is the Avogadro number, and $D_{AB}$ is the mutual diffusion coefficient of the

reactants A (OH radical) and B (NACA). $D_{AB}$ has been calculated from $D_A$ and $D_B$ according to reference [58], and $D_A$ and $D_B$ have been estimated from the Stokes–Einstein approach [59, 60]:

$$D = \frac{k_B T}{6\pi\eta a} \quad (4)$$

where $k_B$ is the Boltzmann constant, $T$ is the temperature, $\eta$ denotes the viscosity of the solvent, in our case, water ($\eta = 8.91 \times 10^{-4}$ Pa s) and benzene ($\eta = 6.04 \times 10^{-4}$ Pa s), and $a$ is the radius of the solute ($a_{OH} = 4.79$ Å and $a_{NACA} = 7.96$ Å).

## 3 Results and discussion

The structure of NACA, as well as the site numbers assigned to each atom in this work, is shown in Fig. 1. As for many other compounds, the antioxidant activity of NACA can take place through different mechanisms [61–64]. For the reaction of NACA with OH radical, they are:

Radical adduct formation (RAF):

$$\mathrm{NACA} + {}^{\cdot}\mathrm{OH} \rightarrow \mathrm{NACA} - \mathrm{OH}^{\cdot}$$

Hydrogen atom transfer (HAT):

$$\mathrm{NACA} + {}^{\cdot}\mathrm{OH} \rightarrow \mathrm{NACA}(-\mathrm{H})^{\cdot} + \mathrm{H_2O}$$

Single electron transfer (SET):

$$\mathrm{NACA} + {}^{\cdot}\mathrm{OH} \rightarrow \mathrm{NACA}^{\cdot+} + \mathrm{OH}^{-}$$

Additionally, SET can occur rapidly followed by, or simultaneously with, proton transfer, which are known as sequential electron proton transfer (SEPT) and proton-coupled electron transfer (PCET), respectively. Even though they yield the same products as HAT, the influence of the solvent on their feasibility is expected to be different. While SET and SEPT are likely to be favored by polar environments that promote solvation of the intermediate ionic species, the PCET might be also viable in non-polar since the transfer of the proton and the electron occurs simultaneously in this case, and therefore, no charged intermediaries are formed.

The free radicals chosen for the present study are ˙OH and ˙OOH. The OH radical has been chosen since it is the most electrophilic [65], and reactive of the oxygen-centered radicals, with a half-life of $\sim 10^{-9}$ s [66]. It can be formed intracellularly by a Fenton-type reaction, by Haber–Weiss recombination, or by other radicals created from enzyme reactions [67–71]. ˙OH radicals can also be produced by ultraviolet and ionizing radiations [72]. Compared with ˙OH, peroxyl radicals are less reactive species capable of diffusing to remote cellular locations

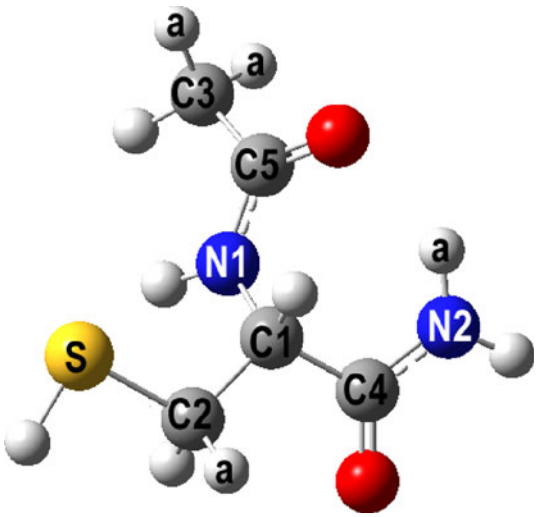


**Fig. 1** Structure and site numbers of NACA

[73]. Their half-lives are of the order of seconds [74], and their electrophilicity is not as high as that of ˙OH [65]. The OOH radical has been chosen since it is the smallest of the family.

According to the structure of NACA, the RAF mechanism could only take place by radical addition to sites C4, C5, N1, and N2. Even though these sites are not expected to readily react this way, the corresponding reactions were modeled to verify such assumption. Most of them were found to be endergonic in both benzene and water solutions for the reaction with ˙OH (Table 1). The only exception is the OH addition to C5 in non-polar environments, which was found to be exergonic by about 4 kcal/mol. Accordingly, only this channel of reaction will be considered for the RAF mechanism. In addition, any attempt to locate the product corresponding to the ˙OH addition to site N1 invariable leads to a non-bonded system that does not correspond to a proper RAF product but to a complex between the two fragments. Since the ˙OOH radical is much less reactive than ˙OH, the only RAF site that was studied was C5, in benzene solution. In this case, this path becomes endergonic by 36.12 kcal/mol. Therefore, the RAF mechanism has been ruled out for the OOH scavenging activity of NACA.

The SET mechanism was also ruled out based on thermochemical considerations. It was found to be endergonic with ΔG values of 102.5 and 31.5 kcal/mol in benzene and water solutions, respectively, for the reaction involving ˙OH. Since it high electrophilicity makes this radical one of the most reactive ROS via SET, this mechanism does not seem to be important for ROS, in general. In line with this reasoning, it was found that the SET reactions involving the OOH radical are even more endergonic (ΔG = 124.6 and 54.7, in benzene and aqueous solutions, respectively). Accordingly, this mechanism is not expected to

**Table 1** Gibbs free energies of reaction for the RAF mechanism of NACA + ·OH reaction

| | ΔG (kcal/mol) | |
|---|---|---|
| | Benzene | Water |
| C4 | 4.02 | 3.54 |
| C5 | −3.96 | 7.93 |
| N1 | 1.78 | 4.54 |
| N2 | 43.83 | 47.73 |

**Table 2** First ionization energy of NACA, in different media and calculated from different approaches

| | Gas | Benzene | Water |
|---|---|---|---|
| Koopman | 10.04 | 8.01 | 7.59 |
| OVGF | 9.25 | 7.23 | 6.84 |
| P3 | 9.13 | 7.10 | 6.70 |
| Vertical | 9.37 | 8.06 | 6.94 |
| Adiabatic | 9.03 | 7.17 | 6.84 |

significantly contribute to the overall antioxidant activity of NACA. This can be due to the large ionization energy (IE) of NACA. To confirm this hypothesis, the IE of NACA has been computed using different approaches. They are as follows:

1. The adiabatic approach, in which the IE of an n-electron system ($X$), calculated at a given level of theory, implies the following energy difference:

$$\mathrm{IP} = E^X_{\mathrm{n-1}}(g_{\mathrm{n-1}}) - E^X_{\mathrm{n}}(g_{\mathrm{n}}) \quad (5)$$

   where $E^X_n(g_{\mathrm{n}})$is the energy of the n-electron neutral system calculated at a geometry $g_{\mathrm{n}}$ and $E^X_{\mathrm{n-1}}(g_{\mathrm{n-1}})$ is the energy of the (n–1)-electron ionic species calculated at a geometry $g_{\mathrm{n-1}}$. Therefore, it takes into account the geometry relaxation of the radical cation after the electron transfer.
2. The vertical approach, where the optimized geometry of the X specie is used to perform the calculation of the radical cation, i.e., no geometry relaxation is included.
3. The Koopmans theorem approximation [75], which is a special case of vertical IE, evaluated as minus the energy of the molecular orbital of the neutral system from which an electron is removed, usually the highest occupied molecular orbital (HOMO).
4. The electron propagator theory (EPT) [76–79], in particular the outer valence Green's function (OVGF) [80–82] and the partial third-order (P3) [83, 84] approximations. They have been successfully applied to a large variety of molecules [85, 86] and are capable of predicting vertical energies within approximately 0.25 eV of the experiments [87].

The values of IE of NACA, obtained from these approaches, are reported in Table 2. There are no experimental reports on the IE of NACA. Therefore, and taking into account that they are usually obtained in gas phase, these values are also included to facilitate possible future comparisons. The values obtained from Koopman's, OVGF, and P3 approaches are proven to be reliable in gas phase, but their accuracy within the continuum solvent models is not clear yet. In addition, they all correspond to vertical energies. Therefore, for obtaining the most accurate possible values of IE in solution, energies of relaxation and solvation have been added to the IEs obtained in vacuum for these three approaches. As the values in Table 2 show, the IEs, in both benzene and water solutions, that are closest to each other are those obtained from the adiabatic and EPT approaches. In general, the agreement among OVGF, P3, and adiabatic values is very good and lower than 0.25 eV, which is the maximum expected error for IEs obtained from EPT. Therefore, they are the recommended values among all the reported ones. In any case, the IE of NACA is high, compared with those of other molecules that react with ROS by SET, and therefore, it seems to be the explanation for the non-viability of this mechanism for the reaction of NACA with OH and probably with other ROS.

Since NACA does not deprotonate under physiological conditions, the SEPT mechanism can only occur by a SET process followed by a proton transfer. Therefore, this mechanism was also ruled out. Thus, from the five mechanisms mentioned at the beginning of this section, only RAF at site C5 (for the reaction with ·OH), HAT, and PCET have not been ruled out so far.

Even though the PCET mechanism is commonly defined as a concerted electron proton transfer that is not HAT, it has been reported that this is a difficult distinction to make and that HAT can be considered a particular case of PCET reactions [88]. In any case, it is important to identify whether the corresponding transition state (TS) structures actually correspond to HAT or PCET mechanisms. To that purpose, an analysis of the electronic density of the singly occupied molecular orbital (SOMO) of each TS has been carried out. Since it is commonly accepted that the PCET mechanism can be defined as that in which the proton and the electron are transferred between different sets of orbitals [89], the analysis of the singly occupied molecular orbital (SOMO) of the TS seems to be a reliable criterion to differentiate between HAT and PCET processes.

The SOMO of HAT TSs is expected to have significant density in atomic orbitals oriented along, or nearly along, the transition vector (donor–H–acceptor). The SOMO of PCET TSs, on the other hand, involve $p$ orbitals that are

orthogonal to the donor–H–acceptor vector [89]. As the plots in Fig. 2 show, the SOMO of all transition states has a node at the migrating H and is mostly localized on the donor–H–acceptor vector, which corresponds to HAT transition states. Therefore, it can be stated that all the H transfer processes studied in this work correspond to HAT mechanism and that it is actually the only mechanism responsible for the ˙OH and ˙OOH scavenging activity of NACA.

The structures of the TSs that correspond to the HAT mechanism, optimized in benzene and water solutions, are shown in Fig. 3a,b respectively. They involve H atoms at sites C1, C2, C3, N1, N2, and S. While in sites C1, N1, and S, there is only one H atom susceptible to be transferred and therefore only one TS structure was located, for sites C2, C3, and N2, two different TSs arise depending on the particular H atom that is transferred, for the reaction with ˙OH. The different arrangements lead to different interactions and therefore to energies that might be significantly different. Accordingly, it is important to consider all of them in the kinetic study. For site C2, TS-C2 shows an H bond-like interaction between the H atom in the OH fragment and the O atom of the carbonyl group involving C4, regardless of the solvent. On the other hand, no stabilizing interaction was found in TS-C2a when optimized in benzene solution, but it is present when the optimization

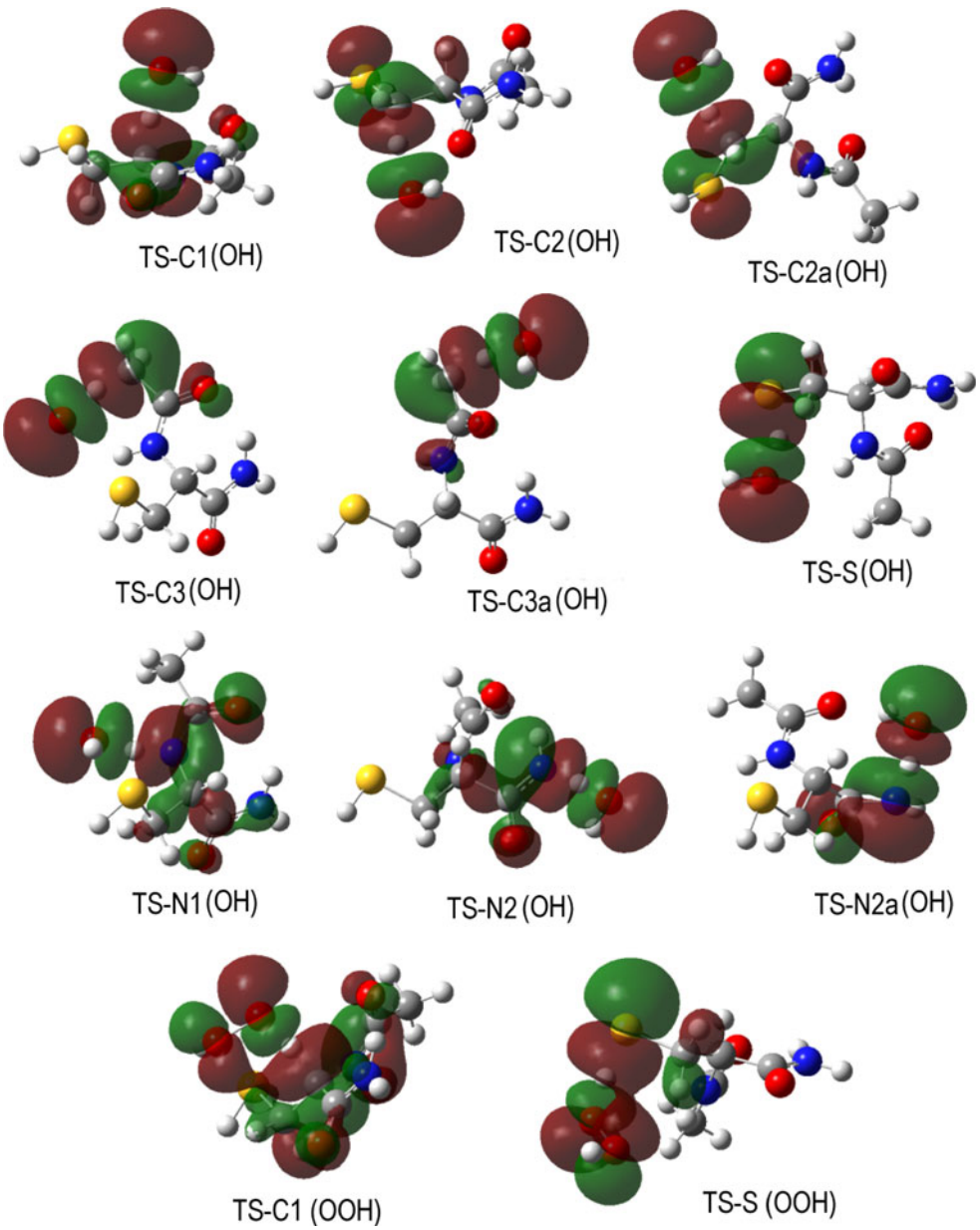


**Fig. 2** SOMO density surfaces of the TS structures, in water solution, computed with an isodensity value of 0.02 au

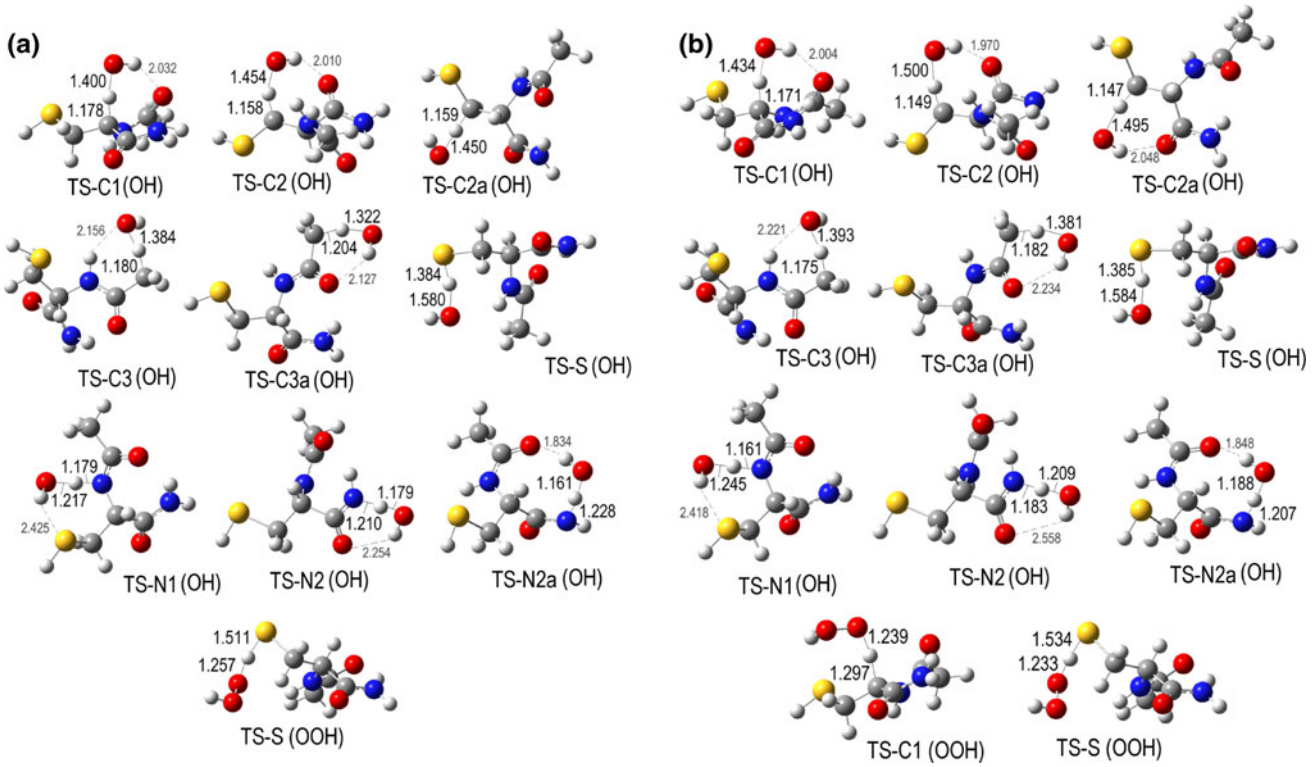


**Fig. 3** **a** Optimized geometries of the transition states involving H transfer processes from sites C1, C2, C3, N1, N2, and S, in benzene solution. **b** Optimized geometries of the transition states involving H transfer processes from sites C1, C2, C3, N1, N2, and S, in water solution

is performed in water solution. For site C3, both transition states show H bond interactions, but while in TS-C3, it involves the O atom of the OH radical and the H atom bonded to N1; in TS-C3a, the interaction involves the H atom in the OH moiety and the O atom bonded to C4. For site N2, both transition states show H bond-like interactions involving the H atom in the OH radical and one of the O atoms in the carbonyl groups of NACA. For TS-N2, the interaction involves the O atom bonded to C4, while for TS-N2a, it involves the O atom bonded to C5. The structural features described for H transfers from C3 to N2 are the same, regardless of the solvent used in the optimization. The fully optimized structures of the transition states corresponding to the NACA + ˙OOH reaction, on the other hand, do not present the interactions described for the TS involving ˙OH.

The Gibbs free energies of reaction (ΔG) obtained for the channels of reactions of the HAT mechanism are reported in Table 3. As these values show, all the studied channels were found to be exergonic for the reactions involving the OH radical, with similar exergonicity in non-polar and polar environments. The largest exergonicity corresponds to H abstractions from the thiol site, which was found to be more than 10 kcal/mol larger than that of the second most exergonic channel, both in polar and in non-polar environments. The ΔG values of the H abstractions from carbon sites were all found to be similar and in the range −20 to 27 kcal/mol in benzene solution and from −22 to 33 in water solution. The least thermochemically favored HAT channels are those corresponding to H abstractions from nitrogen sites, with ΔG values ranging from −2 to 6 kcal/mol. In contrast for the reaction with ˙OOH, most of the reaction channels were found to be endergonic. The exceptions are the H transfer from the SH site both in polar and in non-polar environments and the H transfer from site C1 in aqueous solution. However, this particular path is better described as isoergonic, since its ΔG value is close to zero and smaller than the accuracy of the calculations.

The channels of reaction described as endergonic have been ruled out as relevant to the scavenging activity of NACA. Even if they take place at a significant rate, they would be reversible and therefore the formed products will not be observed. However, it should be noticed that they might still represent significant channels if their products rapidly react further. This would be particularly important if these later stages are sufficiently exergonic to provide a driving force and if their barriers of reactions are low. However, since this work focuses only on the first step of the oxidation of NACA by ˙OH and ˙OOH, the kinetic

**Table 3** Gibbs free energies of reaction (ΔG) and Gibbs free energies of activation ($\Delta G^{\neq}$), in kcal/mol, at 298.15 K

| | NACA + ˙OH | | | | NACA + ˙OOH | | | |
|---|---|---|---|---|---|---|---|---|
| | Benzene | | Water | | Benzene | | Water | |
| | ΔG | $\Delta G^{\neq}$ | ΔG | $\Delta G^{\neq}$ | ΔG | $\Delta G^{\neq}$ | ΔG | $\Delta G^{\neq}$ |
| C1 | −27.41 | 5.86 | −33.16 | 8.13 | 5.21 | | −0.45 | 25.03 |
| C2 | −24.39 | 3.47 | −25.47 | 5.91 | 8.23 | | 7.24 | |
| C2a | | 7.47 | | 6.77 | | | | |
| C3 | −19.81 | 9.07 | −21.70 | 10.61 | 12.81 | | 11.01 | |
| C3a | | 8.52 | | 10.09 | | | | |
| N1 | −8.48 | 11.90 | −9.31 | 16.42 | 24.13 | | 23.39 | |
| N2 | −2.63 | 13.54 | −5.57 | 17.62 | 29.99 | | 27.14 | |
| N2a | | 11.49 | | 15.04 | | | | |
| S | −35.03 | 2.44 | −36.95 | 4.02 | −2.41 | 16.52 | −4.24 | 17.41 |

calculations have been made only for those channels described as exergonic.

The Gibbs free energies of activation ($\Delta G^{\neq}$) were found to be systematically lower in benzene solutions than in water solutions, with the exception of channel C2a, suggesting that from a kinetic point of view, a non-polar environment would favor the scavenging activity of NACA.

For the NACA + ˙OH reaction, the lowest barrier of reaction was found to be that corresponding to HAT from the -SH site, regardless of the polarity of the environment, followed by that of HAT from site C2. In addition, while in non-polar environments, the difference between the two lowest barriers is about 1 kcal/mol, in water solution, such difference was found to be ~2 kcal/mol. This suggests that in the latter case, only H abstraction from the S site would significantly contribute to the overall reactivity of NACA toward OH radicals. The $\Delta G^{\neq}$ value for RAF process involving site C5 in benzene solution, which is the only thermochemically viable RAF channel, is predicted to be ~24 kcal/mol. This is more than 10 kcal/mol higher than any of the HAT channels of reaction in the same medium. Therefore, its contribution to the overall reactivity of NACA toward OH radicals is predicted to be negligible.

Regarding the two exergonic channels of the NACA + ˙OOH reaction, their barriers are significantly higher than those corresponding to the reaction with ˙OH. This is a logical finding based on the relative reactivity of these two free radicals. The channel corresponding to HAT from the –SH site was found to be the one with the lowest barrier. Its $\Delta G^{\neq}$ value is about 8 kcal/mol higher than that of the competing channel (HAT from C1). The barrier of channel S was found to be about 1 kcal/mol lower in non-polar than in polar environments.

Since spin contamination is an issue that can affect the accuracy of energies and structures of open-shell systems, the spin-squared values for all the open-shell species before and after annihilation of the first spin contaminant have been checked, as well as their percent errors with respect to the expected value. These results are provided as Supplementary Material (Tables 1S to 4S). In all cases, the deviations from the ideal value ($\langle S^2 \rangle = 0.75$) were lower than 1.9 and 0.03% before and after annihilation of the first spin contaminant. It has been established that for differences within 10% error, the obtained results can be trusted [90, 91]. Therefore, the spin contamination is negligible for all the radicals species studied in this work, and their energy values are reliable.

The apparent rate constants calculated for all the viable channels of reaction, as well as the overall rate coefficient, are reported in Table 4. It has been assumed that neither mixing nor crossover between different pathways occurs, and therefore, the overall rate coefficient ($k$) has been calculated as the sum of the rate coefficients of each channel:

$$k_{\mathrm{OH}} = k_{\mathrm{app}}^{\mathrm{C1}} + k_{\mathrm{app}}^{\mathrm{C2}} + k_{\mathrm{app}}^{\mathrm{C2}a} + k_{\mathrm{app}}^{\mathrm{C3}} + k_{\mathrm{app}}^{\mathrm{C3}a} + k_{\mathrm{app}}^{\mathrm{N1}} + k_{\mathrm{app}}^{\mathrm{N2}} + k_{\mathrm{app}}^{\mathrm{N2}a} + k_{\mathrm{app}}^{\mathrm{S}} \quad (6)$$

$$k_{\mathrm{OOH}} = k_{\mathrm{app}}^{\mathrm{C1}} + k_{\mathrm{app}}^{\mathrm{S}} \quad (7)$$

According to the overall rate coefficients, NACA is predicted to react with ˙OH about 3 times faster in non-polar media than in aqueous solution. It is also predicted to react with ˙OOH faster in non-polar media than in aqueous solution, but in this case by 1.8 times. The overall reactivity of NACA toward ˙OH radicals was found to be diffusion-controlled in both media, supporting the excellent ˙OH-scavenging activity of NACA. On the contrary, the overall reactivity of NACA toward ˙OOH radicals was found to be rather low. According to the values of the overall rate coefficients reported in Table 4, the efficiency of NACA as OOH radical scavenger is higher than those of melatonin [28] and caffeine [30], slightly lower than that of allicin [92], and significantly lower than that of carotenes [93]. It should be noticed, however, that even when the rate constant for the reaction of NACA with ˙OOH is rather low, it can react faster with other peroxyl radicals in particular with those having substituents with strong electron-accepting character.

The branching ratios of the different reaction channels, which represent the percent of their contribution to the overall reaction, have been calculated as:

$$\Gamma_i = \frac{k_i}{k_{\mathrm{overall}}} \times 100 \quad (8)$$

where $i$ represents each particular channel, i.e., $i$ = C1, C2, C2a, C3, C3a, N1, N2, N2a, or S.

As predicted above based on the barriers of reaction, the OOH-scavenging activity of NACA takes place exclusively

**Table 4** Branching ratios (Γ) and apparent rate constants of the different channels and overall rate coefficient (L $mol^{-1}$ $s^{-1}$), at 298 K

| | NACA + ·OH | | | | NACA + ·OH | | | |
|---|---|---|---|---|---|---|---|---|
| | Benzene | | Water | | Benzene | | Water | |
| | *k* | Γ | *k* | Γ | *k* | Γ | *k* | Γ |
| C1 | 2.67E+08 | 7.04 | 6.80E+06 | 0.50 | 1.06E−03 | ~0 | 1.26E−03 | ~0 |
| C2 | 1.66E+09 | 43.58 | 2.36E+08 | 17.28 | | | | |
| C2a | 5.29E+07 | 1.39 | 6.43E+07 | 4.72 | | | | |
| C3 | 4.32E+06 | 0.11 | 5.00E+05 | 0.04 | | | | |
| C3a | 2.37E+07 | 0.62 | 2.68E+06 | 0.20 | | | | |
| N1 | 2.61E+05 | 0.01 | 2.47E+03 | ~0 | | | | |
| N2 | 3.13E+04 | ~0 | 1.31E+02 | ~0 | | | | |
| N2a | 5.64E+05 | 0.01 | 7.38E+03 | ~0 | | | | |
| S | 1.79E+09 | 47.23 | 1.05E+09 | 77.27 | 1.39E+02 | ~100 | 7.58E+01 | ~100 |
| Overall | 3.80E+09 | | 1.36E+09 | | 1.39E+02 | | 7.58E+01 | |

by H transfer from the SH site, regardless of the polarity of the environment. It was found that when the NACA + ·OH reaction takes place in aqueous solution, HAT from the SH site is the main channel of reaction, with $\Gamma_S = 77.27\%$. The second largest contribution corresponds to HAT from site C2, with $\Gamma_{C2} = 22\%$. The contributions of all the other channels of reactions are negligible in this case. When the reaction occurs in non-polar surroundings, there are two major channels contributing to the overall reactivity of NACA. They are HAT processes from sites S and C2, with $\Gamma_S = 47.23\%$ and $\Gamma_{C2} = 44.97\%$. In this case, channel C1 was also found to contribute to the overall reaction, with small but non-negligible contribution ($\Gamma_{C1} = 7.04\%$). Since OH· is the most reactive radical through HAT, and despite this fact, it is selective for the above-mentioned sites, it can be concluded that all ROS will show at least this selectivity, i.e., those will be the only products expected in the reactions of NACA with any ROS.

## 4 Conclusions

In summary, HAT has been identified as the main mechanism of reaction for the OH and OOH radical scavenging activity of NACA. The overall reactivity of this antioxidant toward OH radicals was found to be diffusion-controlled, regardless of the polarity of the environment. The reactivity of NACA toward OOH, on the other hand, is much lower but still higher than those of melatonin and caffeine. HAT from the S site of NACA is proposed to be the main channel of reaction for the radical scavenging activity of NACA in aqueous solution. On the other hand, it is predicted that sites C2 and S both similarly contribute to the overall reactivity of NACA toward OH radicals in non-polar environments. NACA is predicted to react about 3 times faster in non-polar media than in aqueous solution with ·OH and 1.8 times with ·OOH.

The new insights into the mechanism and kinetics of the NACA + ·OH reaction provided in this work are expected to contribute to the better understanding of the ROS scavenging activity of NACA and related compounds, as well as to the intermediate products formed during their oxidation. Even though this information is primarily useful from an academic point of view, it is also expected to be helpful for practical purposes.

**Acknowledgments** The author thanks Laboratorio de Visualización y Cómputo Paralelo at UAM—Iztapalapa for the access to its computer facilities.

## References

1. Grinberg L, Fibach E, Amer J, Atlas D (2005) Free Radic Biol Med 38:136
2. Penugonda S, Mare S, Goldstein G, Banks WA, Ercal N (2005) Brain Res 1056:132
3. Price TO, Uras F, Banks WA, Ercal N (2006) Exp Neurol 201:193
4. Wu W, Abraham L, Ogony J, Matthews R, Goldstein G, Ercal N (2008) Life Sci 82:1122
5. Zhang X, Banerjee A, Banks WA, Ercal N (2009) Brain Res 1275:87
6. Banerjee A, Zhang X, Manda KR, Banks WA, Ercal N (2010) Free Radic Biol Med 48:1388
7. Sayre LM, Perry G, Smith MA (2008) Chem Res Toxicol 21:172
8. Lin MT, Beal MF (2006) Nature 443:787
9. Reddy PH (2006) J Neurochem 96:1
10. Schoeneich C (2005) Biochim Biophys Acta 1703:111
11. Giasson BI, Ischiropoulos H, Lee VMY, Trojanowski JQ (2002) Free Radic Biol Med 32:1264
12. Aksenov MY, Aksenov MV, Butterfield DA, Geddes JW, Markesbery WR (2001) Neuroscience 163:373
13. Perry G, Raina AK, Nunomura A, Wataya T, Sayre LM, Smith MA (2000) Free Radic Biol Med 28:831

14. Berlett BS, Stadtman ER (1997) J Biol Chem 272:20313
15. Penugonda S, Mare S, Lutz P, Banks WA, Ercal N (2006) Toxicol Appl Pharm 216:197
16. Offen D, Gilgun-Sherki Y, Barhum Y, Benhar M, Grinberg L, Reich R, Melamed E, Atlas D (2004) J Neurochem 89:1241
17. Scott LE, Orvig C (2009) Chem Rev 109:4885
18. Zhao Y, Schultz NE, Truhlar DG (2006) J Chem Theory Comput 2:364
19. Zavala-Oseguera C, Alvarez-Idaboy JR, Merino G, Galano A (2009) J Phys Chem A 113:13913
20. Velez E, Quijano J, Notario R, Pabón E, Murillo J, Leal J, Zapata E, Alarcón G (2009) J Phys Org Chem 22:971
21. Vega-Rodriguez A, Alvarez-Idaboy JR (2009) Phys Chem Chem Phys 11:7649
22. Galano A, Alvarez-Idaboy JR (2009) Org Lett 11:5114
23. Black G, Simmie JM (2010) J Comput Chem 31:1236
24. Furuncuoglu T, Ugur I, Degirmenci I, Aviyente V (2010) Macromolecules 43:1823
25. Galano A, Macías-Ruvalcaba NA, Campos ONM, Pedraza-Chaverri J (2010) J Phys Chem B 114:6625
26. Gao T, Andino JM, Alvarez-Idaboy JR (2010) Phys Chem Chem Phys 12:9830
27. Iuga C, Alvarez-Idaboy J R, Vivier-Bunge A (2011) J Phys Chem A (in press). doi:10.1021/jp201517p
28. Galano A (2011) Phys Chem Chem Phys 13:7147
29. Pérez-González A, Galano A (2011) J Phys Chem B 115: 1306
30. Leon-Carmona JR, Galano A (2011) J Phys Chem B 115:4538
31. Gaussian 09, Revision A.02, Frisch MJ, Trucks GW, Schlegel HB, Scuseria GE, Robb MA, Cheeseman JR, Scalmani G, Barone V, Mennucci B, Petersson GA, Nakatsuji H, Caricato M, Li X, Hratchian HP, Izmaylov AF, Bloino J, Zheng G, Sonnenberg JL, Hada M, Ehara M, Toyota K, Fukuda R, Hasegawa J, Ishida M, Nakajima T, Honda Y, Kitao O, Nakai H, Vreven T, Montgomery Jr JA, Peralta JE, Ogliaro F, Bearpark M, Heyd JJ, Brothers E, Kudin KN, Staroverov VN, Kobayashi R, Normand J, Raghavachari K, Rendell A, Burant JC, Iyengar SS, Tomasi J, Cossi M, Rega N, Millam NJ, Klene M, Knox JE, Cross JB, Bakken V, Adamo C, Jaramillo J, Gomperts R, Stratmann RE, Yazyev O, Austin AJ, Cammi R, Pomelli C, Ochterski JW, Martin RL, Morokuma K, Zakrzewski VG, Voth GA, Salvador P, Dannenberg JJ, Dapprich S, Daniels AD, Farkas Ö, Foresman JB, Ortiz JV, Cioslowski J, Fox DJ (2009) Gaussian Inc., Wallingford
32. Marenich AV, Cramer CJ, Truhlar DG (2009) J Phys Chem B 113:6378
33. Ashcroft RG, Coster HGL, Smith JR (1981) Biochim Biophys Acta 643:191
34. Naumann R, Jonczyk A, Kopp R, van Esch J, Ringsdorf H, Knoll W, Graber P (1995) Angew Chem Int Ed Engl 34:2056
35. Raguse B, Braach-Maksvytis V, Cornell BA, King LG, Osman PDJ, Pace RJ, Wieczorek L (1998) Langmuir 14:648
36. de Heer MI, Mulder P, Korth H–G, Ingold KU, Lusztyk J (2000) J Am Chem Soc 122:2355
37. Pratt DA, Mills JH, Porter NA (2003) J Am Chem Soc 125:5801
38. Gregor W, Grabner G, Adelwohrer C, Rosenau T, Gille L (2005) J Org Chem 70:3472
39. Leopoldini M, Marino T, Russo N, Toscano M (2004) J Phys Chem A 108:4916
40. Nenadis N, Sigalas MP (2008) J Phys Chem A 112:12196
41. Martinez A, Rodriguez-Girones MA, Barbosa A, Costas M (2008) J Phys Chem A 112:9037
42. Okuno Y (1997) Chem Eur J 3:210
43. Benson SW (1982) The foundations of chemical kinetics. Krieger, Malabar
44. Ardura D, Lopez R, Sordo TL (2005) J Phys Chem B 109:23618
45. Alvarez-Idaboy JR, Reyes L, Cruz J (2006) Org Lett 8:1763
46. Alvarez-Idaboy JR, Reyes L, Mora-Diez N (2007) Org Biomol Chem 5:3682
47. Galano A (2007) J Phys Chem A 111:1677
48. Galano A (2008) J Phys Chem C 112:8922
49. Galano A, Cruz-Torres A (2008) Org Biomol Chem 6:732
50. Galano A, Francisco-Márquez M (2008) Chem Phys 345:87
51. Mora-Diez N, Keller S, Alvarez-Idaboy JR (2009) Org Biomol Chem 7:3682
52. Eyring H (1935) J Chem Phys 3:107
53. Evans MG, Polanyi M (1935) Trans Faraday Soc 31:875
54. Truhlar DG, Hase WL, Hynes JT (1983) J Phys Chem 87:2664
55. Eckart C (1930) Phys Rev 35:1303
56. Collins FC, Kimball GE (1949) J Colloid Sci 4:425
57. Smoluchowski M (1917) Z Phys Chem 92:129
58. Truhlar DG (1985) J Chem Ed 62:104
59. Einstein A (1905) Ann Phys Leipzig 17:549
60. Stokes GG (1903) Mathematical and physical papers. Cambridge University Press, Cambridge
61. Galano A, Alvarez-Diduk R, Ramirez-Silva MT, Alarcon-Angeles G, Rojas-Hernandez A (2009) Chem Phys 363:13
62. Chiodo SG, Leopoldini M, Russo N, Toscano M (2010) Phys Chem Chem Phys 12:7662
63. Leopoldini M, Rondinelli F, Russo N, Toscano M (2010) J Agric Food Chem 58:8862
64. Leopoldini M, Russo N, Toscano M (2011) Food Chem 125:288
65. Pryor WA (1988) Free Radic Biol Med 4:219
66. Draganic IG, Draganic ZD (1971) The radiation chemistry of water. Academic Press, New York
67. Sies H (1985) Oxygen stress. Academic Press, London
68. Simic MG, Taylor KA, Ward JF, von Sonntag C (1991) Oxygen radicals in biology and medicine. Plenum Press, New York
69. Davies KJA (1991) Oxidative damage and repair: chemical, biological and medical aspects. Pergamon Press, New York
70. Sies H (1991) Oxygen stress-oxidants and anti-oxidants. Academic Press, London
71. Stadtman ER (1993) Annu Rev Biochem 62:797
72. Von Sonntag C (1987) The chemical basis of radiation biology. Taylor and Francis, London
73. Marnett LJ (1987) Carcinogenesis 8:1365
74. Pryor WA (1986) Annu Rev Physiol 48:657
75. Koopmans T (1933) Physica 1:104
76. Linderberg J, Öhrn Y (2004) Propagators in quantum chemistry, 2nd edn. Wiley-Interscience, Hoboken
77. von Niessen W, Schirmer J, Cederbaum LS (1984) Comput Phys Rep 1:57
78. Herman MF, Freed KF, Yeager DL (1981) Adv Chem Phys 48:1
79. Ortiz JV (1999) Adv Quantum Chem 35:33
80. Zakrzewski VG, Ortiz JV (1994) Int J Quantum Chem 28:23
81. Zakrzewski VG, Ortiz JV (1995) Int J Quantum Chem 53:583
82. Zakrzewski VG, Ortiz JV, Nichols JA, Heryadi D, Yeager DL, Golab JT (1996) Int J Quantum Chem 60:29
83. Ortiz JV (1996) J Chem Phys 104:7599
84. Ferreira AM, Seabra G, Dolgounitcheva O, Zakrzewski VG, Ortiz JV (2001) In: J Cioslowski (ed) Quantum-mechanical prediction of thermochemical data, vol 131. Kluwer, Dordrecht
85. Zakjevskii VV, King SJ, Dolgounitcheva O, Zakrzewski VG, Ortiz JV (2006) J Am Chem Soc 128:13350
86. Zakjevskii VV, Dolgounitcheva O, Zakrzewski VG, Ortiz JV (2007) Int J Quantum Chem 107:2266
87. Flores-Moreno R, Ortiz JV (2009) J Chem Phys 131:124110
88. Mayer JM (2004) Annu Rev Phys Chem 55:363
89. Mayer JM, Hrovat DA, Thomas JL, Borden WT (2002) J Am Chem Soc 124:11142

90. Young D (2001) Computational chemistry: a practical guide for applying techniques to real world problems. Wiley, New York, pp 227–228
91. Allodi MA, Kirschner KN, Shields GC (2008) J Phys Chem A 112:7064
92. Galano A, Francisco-Márquez M (2009) J Phys Chem B 113:16077
93. Galano A, Francisco-Márquez M (2009) J Phys Chem B 113:11338